Water Resources Research

RESEARCH ARTICLE
10.1029/2020WR029009

Key Points:
- Playas are infrequently inundated critical wetland habitats for migratory birds and a source of recharge for the High Plains aquifer
- Modeling playa inundation is challenging but highly valuable for conservation efforts, especially under a changing climate
- Using a convolutional neural network, we can accurately predict monthly inundation for 71,842 playas across the Great Plains

Correspondence to:
K. Solvik,
kylen.solvik@colorado.edu

Citation:
Solvik, K., Bartuszevige, A. M., Bogaerts, M., & Joseph, M. B. (2021). Predicting playa inundation using a long short-term memory neural network. *Water Resources Research*, *57*, e2020WR029009. https://doi.org/10.1029/2020WR029009

Received 10 OCT 2020
Accepted 10 OCT 2021

Predicting Playa Inundation Using a Long Short-Term Memory Neural Network

Kylen Solvik[1,2,3], Anne M. Bartuszevige[4], Meghan Bogaerts[4], and Maxwell B. Joseph[1,2]

[1]North Central Climate Adaptation Science Center, Boulder, CO, USA, [2]Earth Lab, Cooperative Institute for Research in Environmental Sciences (CIRES), University of Colorado, Boulder, CO, USA, [3]Department of Geography, University of Colorado, Boulder, CO, USA, [4]Playa Lakes Joint Venture, Lafayette, CO, USA

Abstract In the Great Plains, playas are critical wetland habitats for migratory birds and a source of recharge for the agriculturally important High Plains aquifer. The temporary wetlands exhibit complex hydrology, filling rapidly via local rain storms and then drying through evaporation and groundwater infiltration. Using a long short-term memory (LSTM) neural network to account for these complex processes, we modeled the probability of playa inundation for 71,842 playas in the Great Plains from 1984 to 2018. At the level of individual playas, the model achieved an F1-score of 0.522 on a withheld test set, displaying the ability to predict complex inundation patterns. When simulating playa inundation over the entire region, the model is able to very closely track inundation trends, even during periods of drought. Our results demonstrate potential for using LSTMs to model complex hydrological dynamics. Our modeling approach could be used to model playa inundation into the future under different climate scenarios to better understand how wetland habitats and groundwater will be impacted by changing climate.

Plain Language Summary Playas are small, rain-fed lakes typically found in the Great Plains of the US. Most of the time, they are dry, but when filled they provide important wetland habitat for migrating birds. As the water drains from the playas, they help to recharge the High Plains aquifer, which provides much of the water for agriculture in the region. We used a machine learning model to predict when individual playas are wet and when they are dry using weather, playa size, and information about the land use adjacent to each playa. Our model can accurately predict when playas fill and drain, valuable information for conservation efforts in the region. This research can be used by conservation managers and land-owners to help protect these critical wetlands.

1. Introduction

Playas are shallow, depressional wetlands in the western Great Plains that are critical wildlife habitats and sources of groundwater recharge (Smith, 2003). They are essential migratory stopover and wintering habitat for wetland-dependent birds in the Central Flyway (Bolen et al., 1989; Davis & Smith, 1998). These temporary wetlands are the lowest point of their own watershed and are filled by intense local precipitation from convective storms. Water is lost through a combination of evapotranspiration and infiltration into the High Plains aquifer (Gurdak & Roe, 2010), a critical and rapidly depleting source of groundwater for agricultural irrigation (Haacker et al., 2016; Steward et al., 2013).

As a result of their semi-arid ecosystem, playas have extended wet-dry cycles, on average only becoming wet once every 11 years (Johnson et al., 2011), but this average masks the wide annual variation in inundation status throughout the region. Furthermore, climate futures for the western Great Plains are warmer, with potential changes in precipitation and humidity that could alter playa hydrology (Ojima et al., 2015; Ojima & Lackett, 2002). Understanding the spatial and temporal patterns of playa inundation—and the ability to predict these patterns into the future—is essential for effective, long-lasting playa conservation. For example, understanding historical patterns of wetness and projecting to the future will allow for targeted conservation to regions that are important now due to their current inundation patterns and regions that will become more important as climate continues to change. Predicting these changes would enable better climate adaptation and risk evaluation for playa-associated wildlife populations.

A variety of previous efforts have focused on predicting inundation as a function of weather, land cover, and other factors (Bartuszevige et al., 2012; Cariveau et al., 2011; Johnson et al., 2011; Uden et al., 2015). For example, Bartuszevige et al. (2012) used a generalized linear mixed model (GLMM) to predict inundation and found positive associations with 14-day precipitation, precipitation variance, playa size, and the slope of surrounding terrain. However, these studies are limited spatially and temporally (both within and among years) and thus extrapolation to the entire playa region or across years is problematic.

Advances in analyzing remotely sensed imagery have allowed scientists to investigate patterns of inundation over longer time periods and broader spatial scales. Research has leveraged Landsat 5 satellite observations to investigate how land cover and land cover change relates to inundation, uncovering longer hydroperiod in urban settings and shorter hydroperiod in croplands, rangelands, and grasslands (Collins et al., 2014; Starr & McIntyre, 2020). Common to many of these efforts is the notion that if we can predict historical inundation status as a function of temperature, precipitation, and spatial context, we may be able to predict future inundation and allow for more effective playa conservation.

Two recent innovations motivate our approach for modeling playa inundation. First, the availability of a long term (1984–2019) monthly water history data set—the JRC Monthly Water History v1.2, hereafter JRC data—provides a novel source of inundation data across the entire playa region (Pekel et al., 2016). Second, the rise of deep learning over the past decade provides new tools for leveraging weather and spatial context to predict playa inundation. In particular, long short-term memory (LSTM) neural networks (Hochreiter & Schmidhuber, 1997), have gained traction in a variety of sequence modeling tasks including natural language processing and time series modeling. Time series applications of LSTMs for hydrology include rainfall-runoff modeling (Kratzert et al., 2018; Li et al., 2020), lake and stream temperature modeling (Daw et al., 2020; Rahmani et al., 2021), soil moisture forecasting (Fang et al., 2017), sewer overflow (Zhang et al., 2018), and more (Shen, 2018). LSTMs account for both long and short range time dependence and nonlinear relationships between inputs and outputs. Because these are neural networks, we can also integrate categorical feature embeddings to mop up residual variation and improve predictive power for observed units (Guo & Berkhahn, 2016).

Here, we present a monthly inundation model across the playa region that builds upon previous inundation work to evaluate how well we can predict inundation as a function of climate, land cover, and playa-specific features. The LSTM model predicts inundation status derived from the intersection of JRC monthly water history with known playas as a function of high resolution historical climate data and land cover. The resulting model provides high-quality monthly predictions of inundation at the playa level while also capturing broad-scale regional patterns in inundation. This provides a key step toward an approach that predicts future inundation status and facilitates more effective playa conservation.

2. Methods

2.1. Data Collection and Preprocessing

The Playa Lakes Joint Venture (PLJV) probable playa data includes 71,842 playa polygons along with key attributes: size, estimated frequency of inundation, distance to the nearest road in feet, and binary flags for if they have been hydrologically modified, if they have been farmed around or through, if they are healthy (playas are considered "healthy" if they are not modified and not farmed around or through), and if they belong to a cluster of playas (PLJV, 2019). The layer also includes the name of the author's organization for each playa (who added it to the database).

For our target variable, we calculated playa inundation for every month of the Landsat-based 30-m JRC Global Surface Water product from March 1984 through December 2018 using Google Earth Engine (Gorelick et al., 2017; Pekel et al., 2016). We defined inundation as containing one or more water pixels, based on the JRC data. The JRC product uses a multi-step expert system to identify water and filter out clouds, shadows, and other bad pixels on a monthly time interval. When there are no valid observations for a given month, the pixel is labeled as water only if it was water in the months before and after. With less than 5% overall errors of omission, the JRC data are highly accurate, but its performance is worse for small water bodies, seasonal water, and/or water with standing vegetation (Pekel et al., 2016). Since many playas meet one or more of these conditions (e.g., 33% of the PLJV playas are smaller than 0.5 ha), the JRC product likely does not capture all inundations. Nevertheless, the data are generally very accurate and is methodologically consistent throughout the time series, and so we decided to proceed with the JRC data. However, our modeling methods are flexible enough to accommodate any calculated inundation time series as the target variable. If better and/or higher resolution surface water data become available in the future, it would be easy to retrain the model using the updated data.

Monthly precipitation, temperature, and vapor pressure deficit (VPD) were obtained from the PRISM Gridded Climate historical data products (PRISM Climate Group, 2020). In the same way we calculated inundation, we extracted monthly weather data for each of the 71,842 playas using Google Earth Engine from 1984 through the end of 2018. This resulted in a time series of 3 weather variables that we could match to the inundation data.

Previous research has shown that the land-use/land-cover (LULC) around a playa can dramatically impact its inundation dynamics (Bartuszevige et al., 2012). To incorporate this into our model, we used modeled and historical USGS LULC data (Sohl et al., 2014, 2016), which is available as a backcasted annual data product from 1938 to 1992 (Sohl, Sayler, et al., 2018), historical data from 1992 to 2005, and future projections for four different emission scenarios from the IPCC's Special Report on Emissions Scenarios (the A1B, A2, B1, and B2 scenarios) from 2005 to 2100 (Sohl, Reker, et al., 2018). For modeling inundation between 2005 and 2018, we used projections from the A1B scenario, which represents a focus on economic growth with a mixture of energy production in a globalized world (Nakicenovic et al., 2000). Since there is very minimal difference between the SRES scenarios between 2005 and 2018 and the overwhelming majority of divergence begins after 2020, scenario selection was not critical for our 1984–2018 time frame. After downloading the data, we extracted the fraction of each land cover type per year within a 200-m buffer of the center point for each playa. We used a random point sampling approach to perform the buffered extraction, generating 5,000 random points within each 200m buffer and then calculating the fraction of those 5,000 that fell within the different LULC classes. This method is efficient and provides accurate estimates of the fraction of the buffer area that falls in each raster pixel, whereas rasterization approaches typically only include or exclude pixels in their entirety based on whether they intersect or majority intersect with the buffer. The code for the randomized buffer extraction is publicly available on GitHub (Solvik, 2021).

In order to capture watershed information, we used the USGS Watershed Boundary Dataset Hydrologic Unit Codes (HUCs). The units are organized into nested levels of detail, such that the largest units (regions or HUC-2 because the code contains two digits) are broken down into successive smaller units: subregions (HUC-4), accounting units (HUC-6), and cataloging units (HUC-8, also known as watersheds). The most recent data further subdivides cataloging units into HUC-10 and HUC-12 codes. We downloaded the Watershed Boundary Data set HUC shapefiles from the USGS website (USDA-NRCS et al., 2020) and performed a spatial join in QGIS to assign each playa to its HUC-8. In total, the playas fell into 140 different HUC-8 watersheds.

2.2. Modeling

For each month in our data, each playa is either inundated with some amount of water (represented as a 1) or not inundated (0). While this binary approach sacrifices the finer detail of fractional inundation measures, it is more robust to errors in the playa polygons and/or surface water data. It also simplifies the modeling problem. Our model was trained to predict probability of inundation on a monthly basis.

These data were split into train, validation, and test sets by year: all observations from 1984 to 2010 (27 years) were placed in the training set, observations from 2011 through 2014 (4 years) were placed in validation, and everything from 2015 to 2018 (4 years) was withheld as the final test set. After splitting the data into train, validation, and test sets, we scaled the numerical inputs to the model (e.g., monthly precipitation) by centering the mean to 0 and scaling to unit variance. The scaler was fit to the train set and then applied to the validation and test sets to avoid any information leakage that would unfairly benefit the model.

We included three categorical variables in the model: playa ID (from 0 to 71,842), HUC-8 code (one of 140 options), and playa data source (or "author", one of 5 author organizations). The first two were used to help to encode differences in inundation dynamics between playas and hydrological units that may not be captured by the continuous variables. The last, the playa data source or "author", represents the organization

Table 1
Input Features for LSTM

Feature category	Feature names
Monthly weather data (3 features)	Temperature, precipitation, vapor pressure deficit (VPD)
PLJV playa attributes (9 features)	Playa area (in acres), mean inundation frequency (1984–2010), distance to road (in feet), saturated thickness of the High Plains aquifer in 2013, and binary flags for whether the playa was: healthy, farmed, hydrologically modified, and/or part of a cluster
Land cover fraction (13 features)	Fraction of each Sohl et al. LULC code: water (1), urban (2), clearcut (3), mining (6), barren (7), deciduous (8), evergreen (9), mixed (10), grassland (11), shrubland (12), cropland (13), pasture (14), wetland (15, 16)
Categorical (3 features, passed through embedding layers)	Playa ID (one of 71,842 values), HUC-8 code (one of 140 values), Author (one of five values)

that provided the playa outline and metadata to the PLJV database. We included it in the model to account for potential small differences in how the author organizations defined and input the playa information. Each of these categorical variables were included via unitless embedding layers of dimension 16 (ID), 8 (HUC-8), or 4 (author). An embedding of dimension D is a matrix that provides a vector of length D for each category. This is a multivariate generalization of "dummy"/indicator variables, which are embeddings of dimension 1. For example, the embedding of playa ID is a matrix with 71,842 rows and $D = 16$ columns. For any one playa, the length 16 vector corresponding to one row can represent features unique to that particular playa. In total, the set of all such vectors can represent features of every particular playa and account for differences that are not explained by other model inputs.

We used pytorch's LSTM implementation (torch.nn.LSTM) with binary cross entropy as the loss function. After experimenting with different network sizes and evaluating performance against the validation set, we settled on a hidden layer with 128 dimensions, an ID embedding with 16 dimensions, HUC-8 embedding with 8 dimensions, and data source/author embedding with 4 dimensions ("author" represents the organization that provided the playa polygon and attributes to the PLJV database). Excluding the embeddings, the input consisted of 25 features (Table 1). The model was trained using the Adam optimizer with a starting learning rate of 0.01 and a multiplicative decay (gamma) of 0.85 every five epochs. Weight regularization was used, with an L2 penalty of 3.0×10^{-16}. When validation loss did not improve for 16 consecutive epochs, training was halted and the model state from the best-performing epoch was saved in order to prevent overfitting. In this case, the model trained for 38 epochs and so the model weights at epoch 22 were saved. The LSTM was trained on an AWS EC2 instance with a single NVIDIA T4 GPU. The model output inundation probabilities for each playa and each month in the data set, but modern neural networks often display overconfidence in probability predictions. To address this, we calibrated the outputs using isotonic regression (Zadrozny & Elkan, 2002). As a baseline for comparison, we also fitted a logistic regression model on the same data, withholding 2014–2018 as a test set for evaluation.

The data processing and modeling code is publicly available on GitHub (Solvik, 2020). The input data are publicly available on figshare (Solvik et al., 2021).

3. Results

3.1. Playa Inundation Record Overview

Of the 71,842 playas in the PLJV probable playas data set, 73% did not have a record of inundation during the 34-year time series generated from JRC surface water data (Figure 1), likely an underestimate of actual inundation frequency. The JRC data have higher omission errors for seasonal water and small water bodies and so it likely overlooks inundation of many of the smaller, ephemeral playas. Out of the playas smaller than the median size (1.09 ha), 94% of them had no record of inundation according to the JRC surface water data. Playas in the southern half of the region (New Mexico, Oklahoma, and Texas) were much more likely to be inundated at least once compared to playas in the north (Colorado, Kansas, and Nebraska). This difference may be explained by the north tending to have smaller (median playa size is 0.78 vs. 1.09 ha in the whole data set) and shallower playas located in croplands (74% farmed versus 63% in the whole data set).

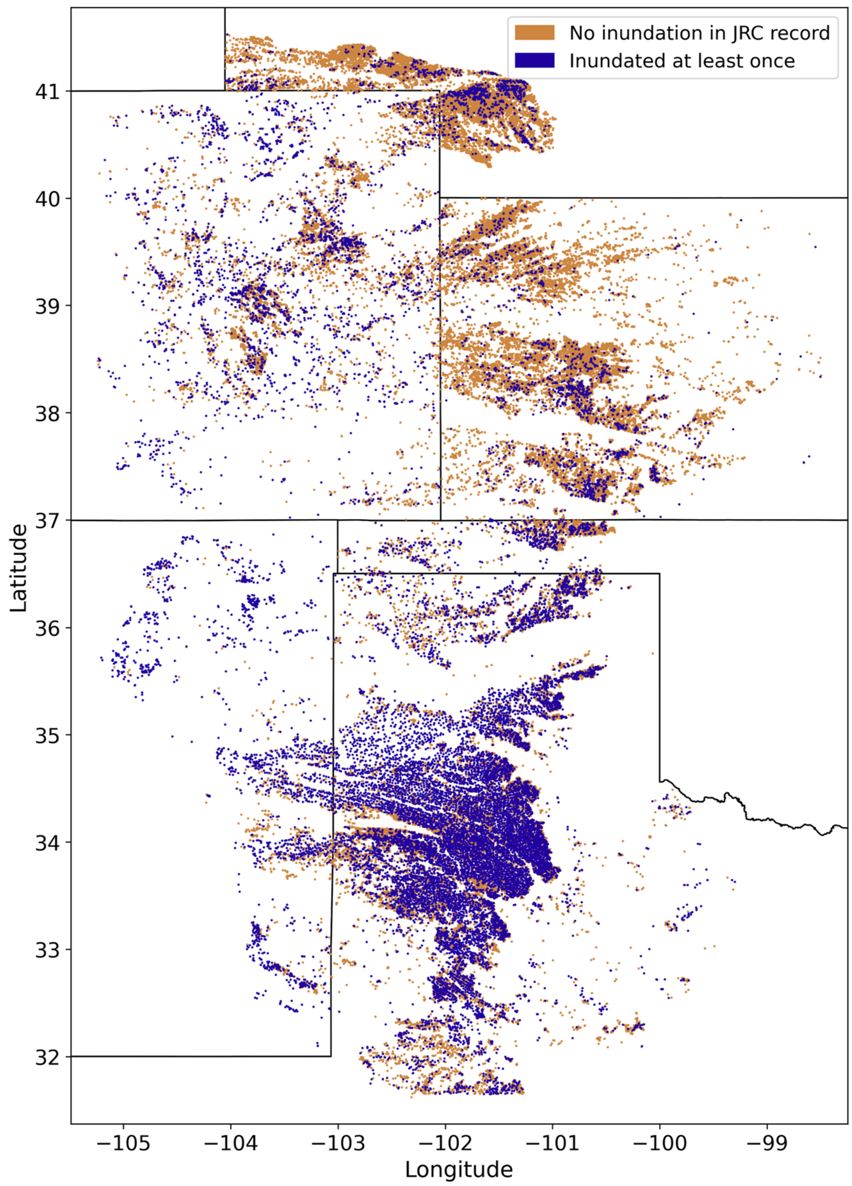

Figure 1. Map of the 71,842 playas in the PLJV data set.

3.2. Overall Model Performance and Probability Calibration Results

The LSTM was able to achieve good performance on the validation and test sets, with F1-scores of 0.491 and 0.522, respectively. Compared to the logistic regression baseline (test $F1 = 0.399$), the LSTM performed much better. Various performance metrics are shown in Table 2 Since accuracy alone is inflated for imbalanced data sets such as ours (where most observations are 0/non-inundated), we consider the other metrics, including AUC and F1-Score, more reliable indicators of model performance. As expected, the model achieved a higher AUC score and better (i.e., lower) loss on the validation set compared to the test, and the Receiving Operating Characteristic curve (ROC curve, Figure 2) shows excellent performance. However, the test set's precision, recall, and F1-scores were all higher than the validation set. This could be due to the drought period during the validation set or a result of the cutoff used to decide whether a prediction was a 1 or 0 (we used 0.25 based on validation F1 performance).

The model displayed some overfitting to the training set ($F1 = 0.644$). After experimenting with various forms and magnitudes of regularization—as well as different initial learning rates and learning rate decay

10.1029/2020WR029009

Table 2
Final Model Performance on Train, Validation, and Test Sets as Well as the Logistic Regression Baseline

	Accuracy	BCE loss	AUC	Precision	Recall	F1-score
Train	0.979	0.0454	0.986	0.581	0.722	0.644
Validation	0.978	0.0464	0.972	0.450	0.541	0.491
Test	0.959	0.0863	0.959	0.474	0.580	0.522
LogReg test (Baseline)	0.944	0.117	0.895	0.334	0.488	0.399

Note. For calculating precision, recall, and F1, a binary cutoff of 0.25 was used (except for the logistic regression baseline, where a cutoff of 0.1 yielded better results).

schedules—we found that an L2 weight penalty of 3.0×10^{-16} and initial learning rate of 0.01 had the best performance on the validation set, despite some overfitting.

Before probability calibration, the model displayed some overconfidence in its inundation probability predictions in the validation and test sets. By using isotonic regression to calibrate the outputs, the actual and predicted inundation probabilities were brought in line (Figure 3), although for the training set the model is slightly underconfident after calibration. Also, the F1-score on the validation and test sets improved slightly (scores in Table 2 are after calibration).

When we look at model performance for individual playas, performance varies. Generally, performance is excellent for playas that had no record of inundation during the 34-year time span, a sign that the playa ID embedding is working well. The model generally can predict inundation well, with consistent accuracy across playa sizes and attributes. The test F1-score was 0.524 for playas smaller than the median size of 1.09 ha and 0.521 for playas larger than the median. Performance was worse for farmed playas (test $F1 = 0.429$) than unfarmed (test $F1 = 0.557$), but better for hydrologically modified playas than unmodified (0.558 vs. 0.499).

To illustrate the LSTM's performance on individual playas, Figure 4 shows the true and predicted inundation time series for 3 playas: the one with the best test loss, the one with the worst, and the one with the median. In the case of the best performing playa, we see that the model ably learns to predict playa inundation, including during the dry validation period and the single inundation spike during the test period (of which the model had no prior knowledge). In the case of the worst, the playa had no record of inundation during the training period and so the model is unable to replicate the sudden inundation pattern that begins in 2014. In the case of the median (and many others), the model identifies most inundation spikes but has a handful of false positives and false negatives throughout.

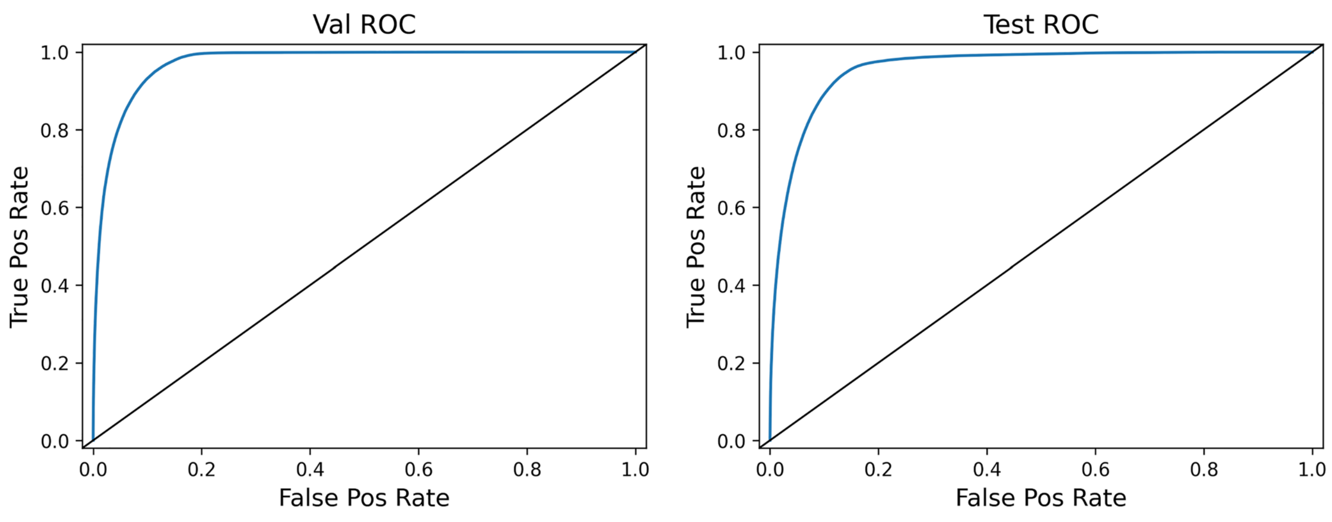

Figure 2. Validation and test set receiver operating characteristic (ROC) curve.

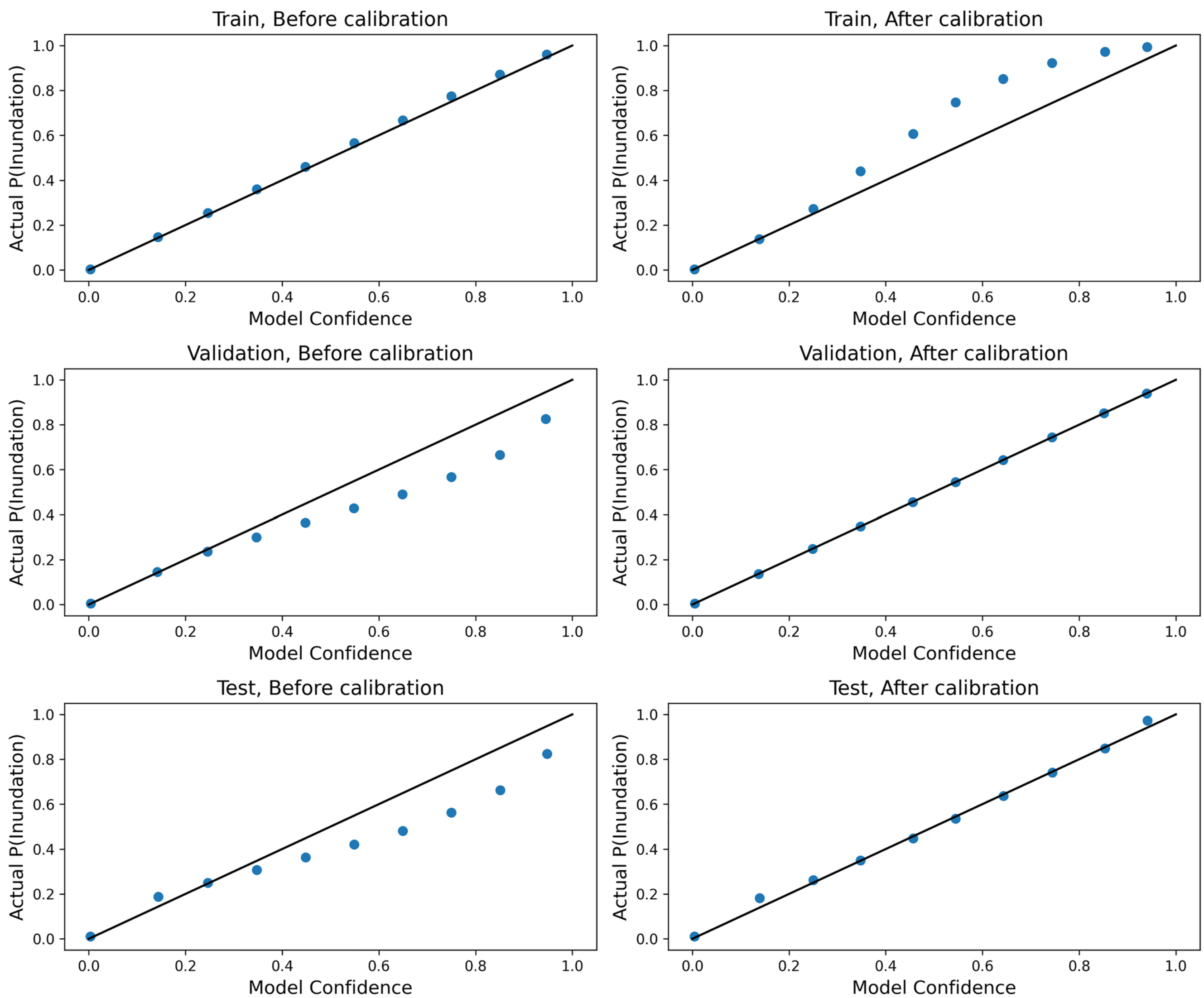

Figure 3. Reliability diagrams for training, validation, and test sets before and after isotonic regression probability calibration. The model's predicted probabilities are binned (0–0.1, 0.1–0.2, etc.) and then the mean probability prediction for each bin is shown on the *x*-axis, while *y*-axis shows the actual proportion of inundation in that bin. Under the 1:1 line represents model overconfidence and above the line represents underconfidence.

Although individual playa performance varies somewhat, the model performs excellently at the regional scale. Figure 5 shows the predicted inundation fraction (the fraction of playas inundated during any given month) for all playas in the data set compared to the ground-truth inundation fraction. The predictions track the ground truth very closely, even during the drought in the validation set (from 2011 to 2013, at its most extreme in 2012) when inundation drops steeply. The accuracy decreases somewhat during the validation and test periods (train RMSE = 0.0059, validation RMSE = 0.0083, and test RMSE = 0.017), but still the predictions match the ground truth well, a sign that the model is able to successfully generalize to unseen data with only modest overfitting. Based on these results, it seems that prediction errors for individual playas average out at the regional scale, producing accurate regional inundation estimations even though the model may over or underestimate inundation for individual playas.

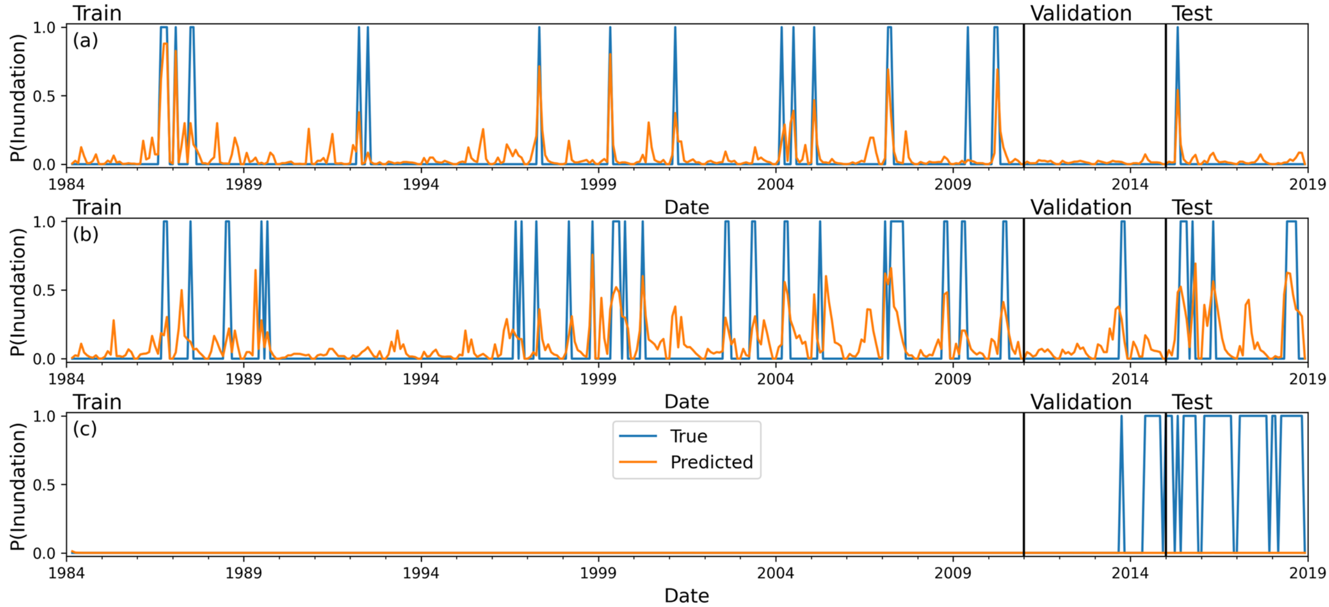

Figure 4. Examples of individual playa inundation versus post-calibration predicted inundation probability timelines. (a) Is the playa with the best test loss (excluding playas without record of inundation), (b) is the playa with the median test loss, and (c) is the playa with the worst.

3.3. Spatial Accuracy

We evaluated the test set loss and F1-score for each playa individually. The results are shown in Figure 6. In the case of playas without record of inundation, an F1-score cannot be calculated and so those were omitted from the map.

In terms of F1, model performance generally is better at the southern end of the range (New Mexico and Texas). This could be due to the higher percentage of playas that had no record of inundation in the north. Based on the HUC and author embeddings, the model likely learned to generally predict less inundation in the north, and so performance is worse for the relatively small percentage of playas in the region that exhibit at least some inundation.

When looking at the loss, that trend seems to reverse: the model performs worse on the playas in Texas and New Mexico than in Nebraska, Kansas, and Colorado. This is also explained by the high concentration of playas without a record of inundation in the north. The model generally handles playas without a record of inundation very well and can more easily learn to predict no inundation throughout their entire time series, which leads to a low (i.e., better) loss. Recall that playas that had no record of inundation are not included in the F1 map, since F1 is not defined if there are no true positives.

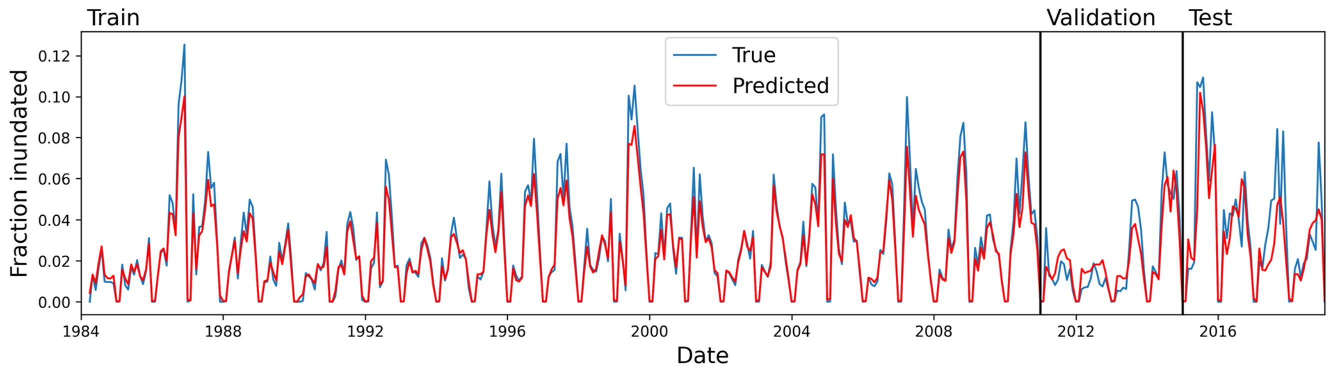

Figure 5. Simulated fraction of playas inundated for each month in the time series.

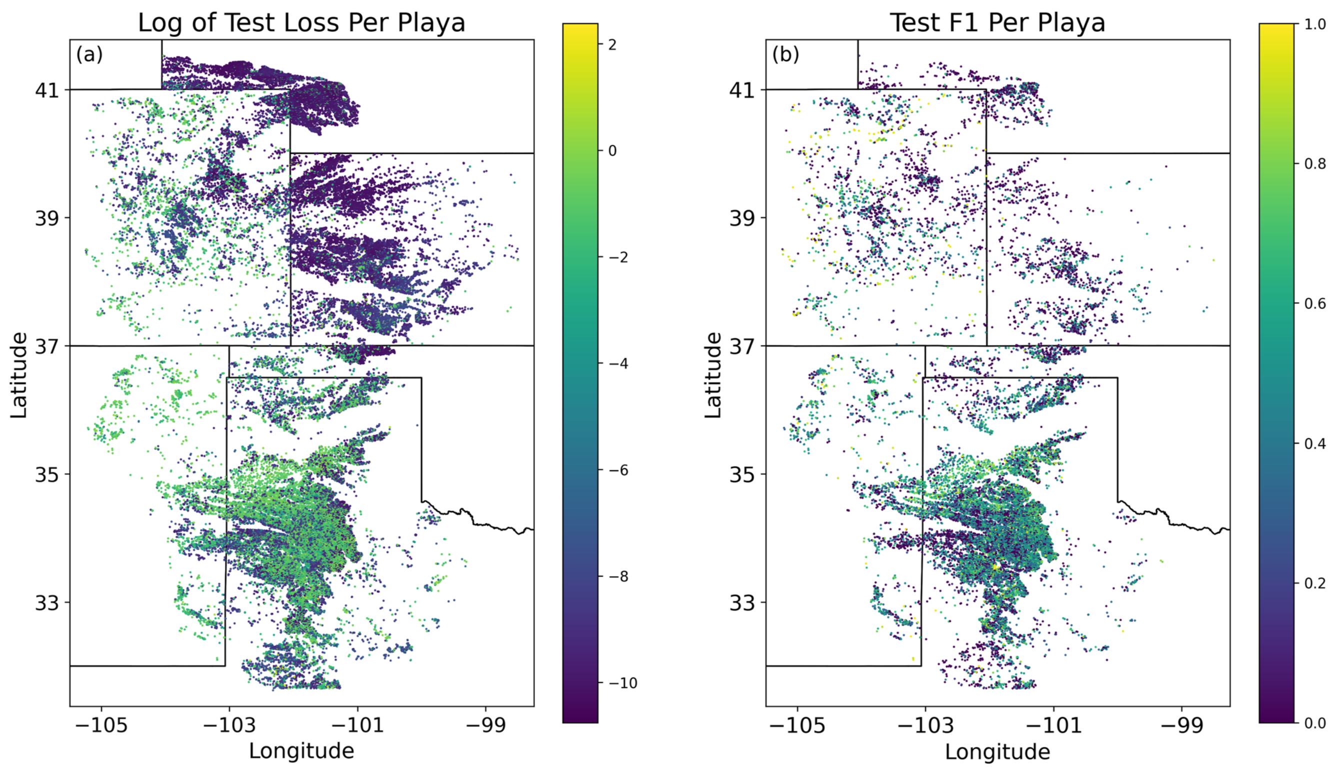

Figure 6. Map of test loss (a) and test F1 scores (b) for each playa. For loss, lower scores (darker colors) are better. For F1, higher scores (lighter colors) are better.

4. Discussion

Overall, the LSTM captures inundation dynamics of individual playas reasonably well and captures inundation at regional scales even better. To our knowledge, no other studies have attempted to model individual playa inundation status on a monthly basis over many years for a large region, but some studies have modeled playa inundation status based on inundation status of other playas at the same point in time (i.e., modeling inundation across playas rather than across time). Uden et al. (2015) used a GLMM to model inundation and ponded area of playas in the Rainwater Basin in south-central Nebraska at two time points (2004 and 2006–2009) as well as using those models to predict playa inundation in 2050. Their binary inundation model yielded a cross-validation AUC score of 0.79 versus our test set AUC of 0.959. While our LSTM model compares favorably, the two modeling problems are not analogous and both time series and time-fixed models can help us understand the current and future conditions of playa wetlands. Because LSTM models are able to capture complex (e.g., nonlinear and nonstationary) dynamics, our approach lends flexibility to hydrological predictions. If sufficient inundation, Meteorological, and landscape data are available, this approach could allow for near term inundation forecasting and playa network time series reconstruction.

We were limited by the resolution and accuracy of available playa, weather, and surface water data. The JRC surface water product has 30-m spatial resolution, which is too large to capture precise playa inundation. Further, due to inconsistent Landsat data availability and its 30-m resolution, the JRC product performs best on large and permanent water bodies that are clear of vegetation (Pekel et al., 2016). Visual inspection of the JRC data showed that it may frequently miss minor inundation events, particularly for smaller playas, playas which are very rarely inundated, and/or those with standing vegetation. This likely explains why such a large percentage of the playas had no record of inundation according to the JRC product during our 34-year time series. A more sensitive playa inundation record could boost our model's performance and value to conservation practitioners. Inundation mapping continues to improve thanks to the application of new techniques and technologies, including LiDAR (Huang et al., 2014). Tang et al. demonstrated that applying a threshold to Tasseled Cap Wetness-Greenness Difference can effectively detect playa inundation in Nebraska (Tang et al., 2016), but obtaining high quality, high resolution, and monthly imagery across the entire western Great Plains is challenging. The PLJV is currently developing a surface water classification approach specifically for detecting playa wetness. When that or another higher resolution surface water data product becomes available, it would be easy to retrain our playa model on new inundation data. This would likely produce more accurate inundation predictions, especially for smaller, more ephemeral playas.

The relatively coarse resolution of the JRC data was one reason why we decided to model inundation as a binary variable: no inundation versus at least partial inundation. We originally planned to model inundation as a continuous fraction between 0 (no inundation) and 1 (fully inundated), but the LSTM frequently diverged during training when attempting to model the continuous fraction. Modeling binary inundation proved to be much more stable, and at 30m resolution the JRC surface water was unlikely to capture small changes in inundation fraction anyways. However, binary inundation predictions are less detailed than continuous inundation fraction predictions, especially for large playas where even a 10% difference in inundated area could indicate a sizable difference in water volume. Nevertheless, our binary approach provides playa conversation planners with the most essential information: whether any part of the playa is likely to be wet during a given month.

The LULC and climate data were also limited by their spatial resolution (500 m for the Sohl et al. LULC data and 4 km for the PRISM climate product). In the case of the LULC data, the land cover immediately surrounding a playa has important effects on inundation (Bartuszevige et al., 2012). With a 500m resolution, the Sohl et al. data may not fully capture variations in LULC near playas. The PRISM climate data do not capture localized rain storms, which may contribute to playa inundation. Further, many playas could fall within the same 4 km PRISM grid cell. Higher resolution LULC and climate data would likely boost model performance. Additionally, the LSTM can only model inundation of playas identified in the PLJV probable playas data set and if there are unmapped playas, our approach cannot capture their inundation patterns until they are added to the data set.

To examine the extent to which our study period affected modeling results, we reran the model using earlier validation and test sets: 2003–2006 and 2007–2010, respectively (instead of 2011–2014 and 2015–2018). This left 1984–2002 (18 years) available as training data, leaving us about 30% less training data than from the full 1984–2010 period (26 years) we used in the main model. The test F1-Score was 0.485, which is lower than the test F1 for the full model (0.522). However, the smaller training data set size (about 30% smaller) may explain this difference, since less training data typically makes for a worse model.

Although the LSTM exhibited good performance, there are limitations associated with black box deep learning methods. First, neural networks in general and LSTMs in particular are not as easy to interpret as more traditional time series models. For example, LSTMs do not readily permit interpretable coefficients that represent the effect of precipitation, temperature, etc. On the model's predictions. Where other modeling approaches, such as the generalized linear mixed model used by Uden et al. (2015), can provide us with more specific insight on the physical drivers of playa inundation, neural networks are comparatively inscrutable, but often very effective as shown here. Neural network interpretability is a crucial and constantly advancing field of research. Second, this model accounts for unmodeled heterogeneity among playas using playa ID embeddings: learned vector representations that allow the model behavior to vary from playa to playa. These embeddings are learned using training data, and in a time series setting the training data consist of historical observations. In a prediction setting, if the hydrology of a playa abruptly changes due to modification in the future, embeddings may not capture subsequent inundation dynamics because they are learned using historical data. Finally, no hydrological dynamics are included in the model. A physics-guided approach that constrains the LSTM with a science-based dynamical model of inundation might allow for a compromise between the flexibility of a neural network, and the physical consistency of a science-based hydrological model (e.g., Karpatne et al., 2018).

This work points to a number of future directions that could inform habitat conservation in the playas region. Conservation has been shown to improve playa wetland health (Zhang et al., 2020) but, given the vastness of the western Great Plains, prioritizing where to focus conservation and restoration efforts can be challenging. Using future projections of climate and land cover data, this model could be used to predict inundation futures at the individual playa and regional scales, which can be used together to plan conservation efforts, particularly in combination with previous results that indicate the importance of maintaining a network of healthy playas (Albanese & Haukos, 2017). These inundation futures are important for understanding how warmer climate futures and/or land cover change might alter inundation, groundwater recharge, and availability of critical playa wetland habitat for migratory birds in the Central Flyway (Gitz & Brauer, 2016; Sohl, 2014; Sohl et al., 2012; Starr & McIntyre, 2020). Beyond availability, connectivity is also important for these critical wetlands, and inundation futures could be used to understand the range of spatiotemporal network dynamics (McIntyre & Strauss, 2013).

5. Conclusions

Playas are critical wetland habitats in the Great Plains, and predicting inundation as a function of land cover, playa characteristics, and climate is important for understanding regional hydrology and wildlife habitat availability. Using an LSTM and a monthly historical record over three decades, we demonstrate that data-driven prediction of future inundation status is possible and may exhibit particularly good performance at a regional scale, with a spectrum of results for individual playas.

Conflict of Interest

The authors declare no conflicts of interest relevant to this study.

Data Availability Statement

The data set for this research is available on figshare (Solvik et al., 2021) under the Creative Commons BY 4.0 license: https://doi.org/10.6084/m9.figshare.13017650.v2.

Acknowledgments
The authors thank Earth Lab at University of Colorado Boulder for technical and computing support and the staff of the North Central Climate Adaptation Science Center for their feedback on the research. This research was funded by Cooperative Agreement No. G18AC00325 from the U.S. Geological Survey North Central Climate Adaptation Science Center (NC CASC). This work was also made possible by the University of Colorado Boulder Grand Challenge initiative and the Cooperative Institute for Research in the Environmental Sciences through their investment in Earth Lab. The authors thank the associate editor and two anonymous reviewers for their valuable comments.

References

Albanese, G., & Haukos, D. A. (2017). A network model framework for prioritizing wetland conservation in the Great Plains. *Landscape Ecology*, *32*(1), 115–130. https://doi.org/10.1007/s10980-016-0436-0

Bartuszevige, A., Pavlacky, D., Jr, Burris, L., & Herbener, K. (2012). Inundation of Playa wetlands in the Western Great Plains relative to landcover context. *Wetlands*, *32*, 1103–1113. https://doi.org/10.1007/s13157-012-0340-6

Bolen, E. G., Smith, L. M., & Schramm, H. L., Jr. (1989). Playa Lakes: Prairie wetlands of the Southern High Plains: The shallow circular basins can provide localized sites of ecological diversity. *BioScience*, *39*(9), 615–623. https://doi.org/10.2307/1311091

Cariveau, A. B., Pavlacky, D. C., Bishop, A. A., & LaGrange, T. G. (2011). Effects of surrounding land use on playa inundation following intense rainfall. *Wetlands*, *31*(1), 65–73. https://doi.org/10.1007/s13157-010-0129-4

Collins, S. D., Heintzman, L. J., Starr, S. M., Wright, C. K., Henebry, G. M., & McIntyre, N. E. (2014). Hydrological dynamics of temporary wetlands in the southern Great Plains as a function of surrounding land use. *Journal of Arid Environments*, *109*, 6–14. https://doi.org/10.1016/j.jaridenv.2014.05.006

Davis, C. A., & Smith, L. M. (1998). Ecology and management of migrant shorebirds in the Playa Lakes Region of Texas. *Wildlife Monographs*, 3–45.

Daw, A., Thomas, R. Q., Carey, C. C., Read, J. S., Appling, A. P., & Karpatne, A. (2020). Physics-guided architecture (PGA) of neural networks for quantifying uncertainty in lake temperature modeling. In *Proceedings of the 2020 SIAM international conference on data mining* (pp. 532–540). Society for Industrial and Applied Mathematics. https://doi.org/10.1137/1.9781611976236.60

Fang, K., Shen, C., Kifer, D., & Yang, X. (2017). Prolongation of SMAP to spatiotemporally seamless coverage of continental U.S. using a deep learning neural network. *Geophysical Research Letters*, *44*(21), 11–11. https://doi.org/10.1002/2017GL075619

Gitz, D., & Brauer, D. (2016). Trends in Playa Inundation and water storage in the Ogallala Aquifer on the Texas High Plains. *Hydrology*, *3*(3), 31. https://doi.org/10.3390/hydrology3030031

Gorelick, N., Hancher, M., Dixon, M., Ilyushchenko, S., Thau, D., & Moore, R. (2017). Google Earth Engine: Planetary-scale geospatial analysis for everyone. *Remote Sensing of Environment*, *202*, 18–27. https://doi.org/10.1016/j.rse.2017.06.031

Guo, C., & Berkhahn, F. (2016). *Entity embeddings of categorical variables*. ArXiv:1604.06737 [Cs]. Retrieved from http://arxiv.org/abs/1604.06737

Gurdak, J. J., & Roe, C. D. (2010). Recharge rates and chemistry beneath playas of the High Plains aquifer, USA. *Hydrogeology Journal*, *18*(8), 1747–1772. https://doi.org/10.1007/s10040-010-0672-3

Haacker, E. M. K., Kendall, A. D., & Hyndman, D. W. (2016). Water level declines in the high plains aquifer: Predevelopment to resource senescence. *Groundwater*, *54*(2), 231–242. https://doi.org/10.1111/gwat.12350

Hochreiter, S., & Schmidhuber, J. (1997). Long short-term memory. *Neural Computation*, *9*(8), 1735–1780. https://doi.org/10.1162/neco.1997.9.8.1735

Huang, C., Peng, Y., Lang, M., Yeo, I.-Y., & McCarty, G. (2014). Wetland inundation mapping and change monitoring using Landsat and airborne LiDAR data. *Remote Sensing of Environment*, *141*, 231–242. https://doi.org/10.1016/j.rse.2013.10.020

Johnson, W. P., Rice, M. B., Haukos, D. A., & Thorpe, P. P. (2011). Factors influencing the occurrence of inundated playa wetlands during winter on the Texas high plains. *Wetlands*, *31*(6), 1287–1296. https://doi.org/10.1007/s13157-011-0243-y

Karpatne, A., Watkins, W., Read, J., & Kumar, V. (2018). *Physics-guided neural networks (PGNN): An application in lake temperature modeling*. Retrieved from http://arxiv.org/abs/1710.11431. ArXiv:1710.11431 [Physics, Stat].

Kratzert, F., Klotz, D., Brenner, C., Schulz, K., & Herrnegger, M. (2018). Rainfall–runoff modelling using long short-term memory (LSTM) networks. *Hydrology and Earth System Sciences*, *22*(11), 6005–6022. https://doi.org/10.5194/hess-22-6005-2018

Li, W., Kiaghadi, A., & Dawson, C. N. (2020). High temporal resolution rainfall runoff modelling using long-short-term-memory (LSTM) networks. *Neural Computing & Applications*, *33*, 1261–1278. https://doi.org/10.1007/s00521-020-05010-6

McIntyre, N. E., & Strauss, R. E. (2013). A new, multi-scaled graph visualization approach: An example within the playa wetland network of the Great Plains. *Landscape Ecology*, *28*(4), 769–782. https://doi.org/10.1007/s10980-013-9862-4

Nakicenovic, N., Alcamo, J., Grubler, A., Riahi, K., Roehrl, R., Rogner, H.-H., & Victor, N. (2000). *Special Report on emissions scenarios (SRES): A special Report of working Group III of the intergovernmental panel on climate change*. Cambridge University Press.

Ojima, D., Steiner, J., McNeeley, S., Cozzetto, K., & Chilss, A. (2015). *Great Plains regional technical input report* (224). Springer.

Ojima, D. D., & Lackett, J. M. (2002). *Preparing for a changing climate: The potential consequences of climate variability and change—central Great Plains*. Colorado State University.

Pekel, J.-F., Cottam, A., Gorelick, N., & Belward, A. S. (2016). High-resolution mapping of global surface water and its long-term changes. *Nature*, *540*(7633), 418–422. https://doi.org/10.1038/nature20584

PLJV. (2019). *Probable playas data layer*. Retrieved from https://pljv.org/for-habitat-partners/maps-and-data/data-downloads/

PRISM Climate Group. (2020). *PRISM climate data*. Retrieved from http://prism.oregonstate.edu

Rahmani, F., Lawson, K., Ouyang, W., Appling, A., Oliver, S., & Shen, C. (2021). Exploring the exceptional performance of a deep learning stream temperature model and the value of streamflow data. *Environmental Research Letters*. https://doi.org/10.1088/1748-9326/abd501

Shen, C. (2018). A transdisciplinary review of deep learning research and its relevance for water resources scientists. *Water Resources Research*, *54*(11), 8558–8593. https://doi.org/10.1029/2018WR022643

Smith, L. M. (2003). *Playas of the great plains* (Vol. 3). University of Texas Press.

Sohl, T., Reker, R., Bouchard, M., Sayler, K., Dornbierer, J., Wika, S., et al. (2016). Modeled historical land use and land cover for the conterminous United States. *Journal of Land Use Science*, *11*(4), 476–499. https://doi.org/10.1080/1747423X.2016.1147619

Sohl, T. L. (2014). The relative impacts of climate and land-use change on conterminous United States bird species from 2001 to 2075. *PLoS One*, *9*(11), e112251. https://doi.org/10.1371/journal.pone.0112251

Sohl, T. L., Reker, R. R., Bouchard, M. A., Sayler, K. L., Dornbierer, J., Wika, S., et al. (2018). *Conterminous United States land cover projections - 1992 to 2100 [data set]*. U.S. Geological Survey. https://doi.org/10.5066/P95AK9HP

Sohl, T. L., Sayler, K. L., Bouchard, M. A., Reker, R. R., Friesz, A. M., Bennett, S. L., et al. (2014). Spatially explicit modeling of 1992–2100 land cover and forest stand age for the conterminous United States. *Ecological Applications*, *24*(5), 1015–1036. https://doi.org/10.1890/13-1245.1

Sohl, T. L., Sayler, K. L., Bouchard, M. A., Reker, R. R., Friesz, A. M., Bennett, S. L., et al. (2018). *Modeled historical land use and land cover for the conterminous United States: 1938-1992 [data set]*. U.S. Geological Survey.

Sohl, T. L., Sleeter, B. M., Sayler, K. L., Bouchard, M. A., Reker, R. R., Bennett, S. L., et al. (2012). Spatially explicit land-use and land-cover scenarios for the Great Plains of the United States. *Agriculture, Ecosystems and Environment*, *153*, 1–15. https://doi.org/10.1016/j.agee.2012.02.019

Solvik, K. (2020). *Kysolvik/raster-buffer-extract* (Version v0.1.1). https://doi.org/10.5281/zenodo.4044086

Solvik, K., (2021). *Kysolvik/playa-inundation* (Version v1.0.1). https://doi.org/10.5281/zenodo.5655759

Solvik, K., Bartuszevige, A., Bogaerts, M., & Joseph, M. (2021). Playa inundation CNN pre-processed input (Version 2). https://doi.org/10.6084/m9.figshare.13017650.v2

Starr, S. M., & McIntyre, N. E. (2020). Land-cover changes and influences on playa wetland inundation on the Southern High Plains. *Journal of Arid Environments*, *175*, 104096. https://doi.org/10.1016/j.jaridenv.2019.104096

Steward, D. R., Bruss, P. J., Yang, X., Staggenborg, S. A., Welch, S. M., & Apley, M. D. (2013). Tapping unsustainable groundwater stores for agricultural production in the High Plains Aquifer of Kansas, projections to 2110. *Proceedings of the National Academy of Sciences*, *110*(37), E3477–E3486. https://doi.org/10.1073/pnas.1220351110

Tang, Z., Li, Y., Gu, Y., Jiang, W., Xue, Y., Hu, Q., et al. (2016). Assessing Nebraska playa wetland inundation status during 1985–2015 using Landsat data and Google Earth Engine. *Environmental Monitoring and Assessment*, *188*(12), 654. https://doi.org/10.1007/s10661-016-5664-x

Uden, D. R., Allen, C. R., Bishop, A. A., Grosse, R., Jorgensen, C. F., LaGrange, T. G., et al. (2015). Predictions of future ephemeral springtime waterbird stopover habitat availability under global change. *Ecosphere*, *6*(11), art215. https://doi.org/10.1890/es15-00256.1

USDA-NRCS, USGS, & EPA. (2020). *Watershed boundary dataset*. Retrieved from http://datagateway.nrcs.usda.gov

Zadrozny, B., & Elkan, C. (2002). Transforming classifier scores into accurate multiclass probability estimates. *Proceedings of the Eighth ACM SIGKDD International Conference on Knowledge Discovery and Data Mining*, 694–699. https://doi.org/10.1145/775047.775151

Zhang, D., Lindholm, G., & Ratnaweera, H. (2018). Use long short-term memory to enhance Internet of Things for combined sewer overflow monitoring. *Journal of Hydrology*, *556*, 409–418. https://doi.org/10.1016/j.jhydrol.2017.11.018

Zhang, H., Tang, Z., Bishop, A., Drahota, J., LaGrange, T., & Varner, D. (2020). Conservation significantly improves wetland conditions: Evaluation of playa wetlands in different conservation status. *Wetlands Ecology and Management*, *28*(1), 85–102. https://doi.org/10.1007/s11273-019-09696-x